Effects of Partial Edge Loading and Fibre Configuration on Vibration and Buckling Characteristics of Stiffened Composite Plates

Abstract

In this work, the influence of uniaxial and biaxial partial edge loads on buckling and vibration characteristics of stiffened laminated plates is examined by using finite element method. As the initial pre-buckling stress distributions within an element are highly non-uniform in nature for a given loading and edge conditions, the critical loads are evaluated by dynamic approach. Towards this, a nine-node heterosis plate element and a compatible three-node beam element are developed by employing the effect of shear deformation for both the plate and the stiffeners respectively. In the structural modeling, the plate and the stiffener elements are treated separately, and then the displacement compatibility is maintained between them by using a transformation matrix. Effect of different parameters such as loaded edge width, position of loads, boundary conditions, ply-orientations and stiffener factors are considered in this study. Buckling results show that the uniaxial loaded stiffened plate with around $(+30^{o}/-30^{o})_2$ layup can withstand higher load irrespective of boundary conditions and loading patterns, whereas the maximum load resisting layup for the biaxially loaded stiffened plate is purely dependent on edge conditions and loading patterns.

T. Rajanna [a,*]
Sauvik Banerjee [b]
Yogesh M. Desai [c]
D. L. Prabhakara [d]

[a] Research Scholar, [b] Associate Professor, [c] Professor, Department of Civil Engineering Indian Institute of Technology Bombay, Mumbai-400 076, India
[d] Director, Sahyadri College of Engineering and Management, Mangalore-575 007, India

[*] Assistant Professor, Department of Civil Engineering, B.M.S. College of Engineering (Autonomous College under VTU), Bengaluru-560 019, India

E-mails: [a] t.rajanna@gmail.com
[b] sauvik@civil.iitb.ac.in
[c] desai@civil.iitb.ac.in
[d] cacep2001@yahoo.com

1 INTRODUCTION

Composite laminates belong to a category of thin-walled structures that are commonly being used in many applications like aerospace, civil, marine, and mechanical engineering structures. These laminates have been extensively used in weight sensitive aircrafts and aerospace industries since their inception, and recently in civil engineering structures such as bridge decks, bridge girders, strengthening and retrofitting of existing structures.

Higher strength/weight ratio, high specific stiffness, enhanced fatigue life are some of the well-known characteristics of composite materials. These characteristics are further enhanced by adding stiffener to a plate without considerably affecting its overall weight. For a negligible weight penalty, there is an enormous increase in the strength and stability characteristics throughout the structures.

Plates with an array of stiffeners are commonly found in fuselage and wings of an aircraft, a ship's hull and its deck, offshore drilling rigs, pressure vessels, roofing units, launching pedestal of rocket, etc. The diverse applications of such stiffened plates are found to be exposed to in-plane edge loading in many situations. The presence of these loadings may significantly alter the free vibration response of such stiffened plates. In fact, a situation may arise wherein the natural frequency of a component becomes zero, thereby causing instability of the component at a fairly low-stress field. Hence, the problem of elastic stability may be considered as a special case of vibration problems, and such problems are of considerable importance and interest to researchers for many years.

Many past studies have reported on stability and/or vibration characteristics of stiffened/unstiffened plates with uniform compressive edge loads (Kamruzzaman et al., 2006; Khedmati and Edalat, 2010; Mirzaei et al., 2015; Sayyad and Ghugal, 2014; Sayyad et al., 2016; Singh and Chakrabarti, 2012). However, such uniform edge compressions are unusual in practice. Many practical situations demand the stiffened plate subjected to concentrated and partial edge loads.

The problem of elastic stability of a simply supported plate with in-plane concentrated loads acting opposite to each other was first attempted by Sommerfield (1906). The results were based on simplified approximate plane stress analysis and hence lead to a considerable error. Yamaki (1953) obtained the buckling loads for a simply supported plate with partially distributed edge loads by employing assumptions similar to Sommerfield (1906). Leissa and Ayoub (1988) investigated the vibration and stability of circular and rectangular plates under concentrated edge loads acting opsite to each other using Ritz method. They utilized finite element and plane elasticity solutions for obtaining the initial pre-buckling stresses, and they were the first to analyze vibration characteristics under concentrated forces. Kaldas and Dickinson (1981) also employed Rayleigh-Ritz technique to study the vibration and stability behaviour of thin plates with complicated pre-buckled stress distribution. Jana and Bhaskar (2006) examined the effect of different edge loads on stability beiour of plates using a semi-analytical method. The initial in-plane stresses were found by using Airy's stress function and extended Kantorovich technique. The critical loads were hence determined by Galerkin's method. Hashemi et al. (2008) have contributed analytical solutions for the stability behaviour of isotropic plate under uni-/bidirectional in-plane compressive edge loadings. Deolasi et al. (1995) have employed finite element (FE) technique for analyzing the buckling and vibration problems of plates with different edge loading conditions. Singh et al. (2012) imparted some buckling results for rectangular plates under different non-uniform edge load distributions using FE technique. Stability behaviour of clamped and simply supported square laminated plates

under uni-/bidirectional partial edge loading conditions using FE method was investigated by Sundaresan et al. (1998). The same problem was further explored by Sahu et al. (2001) with an extension to the vibration behaviour of laminated plates under different edge loads. Srivastava et al. (2003) examined the critical buckling behaviour of isotropic stiffened plates with partial and contrated loads using FE approach. The free vibration characteristics of isotropic stiffened plates are studied by Hamedani et al. (2012) using super finite element technique. The same problem and techniques were further extended to get buckling results by Hamedani and Ranji (2013).

It has been observed that, in finite element formulation, most of the authors have used eight-node serendipity elements by considering the effect of shear deformation. Some authors (Palani et al., 1989; Palani et al., 1992; Pugh et al., 1978) have noticed that for certain mesh configuration boundary conditions, the eight-node plate element locks in shear, even when selective or reduced integration techniques are used for a thin plate configuration. It is also stated that the eight-node serendipity element is comparatively more sensitive to element aspect ratios and element shape distortions (Palani et al., 1989) whereas, the nine-node Lagrange element exactly interpolates the quadratic displacement fields and has nearly optimal performance (Palani et al., 1989; Pugh et al., 1978). However, some of the authors (Butalia et al., 1990; Hughes and Cohen, 1978) have also found that the nine-node Lagrange element locks in shear, even when reduced or selective integration techniques are employed for thin plates. In fact, the stiffness matrix exhibits rank deficiency resulting in the appearance of spurious mechanisms, i.e. zero energy modes (Butalia et al., 1990; Hinton and Owen, 1984; Hughes and Cohen, 1978). These communicable mechanisms may result in erratic solution. These shortcomings, namely locking and spurious mechanisms, have led to the development of a heterosis element by employing serendipity shape functions for transverse degree of freedom w, and Lagrange shape functions for rotations θ_x and θ_y (Butalia et al., 1990; Hughes and Cohen, 1978). This element exhibits improved characteristics as compared to each of the previous quadratic elements and offers high accuracy for extremely thin plate configuration (Hughes and Cohen, 1978). The same element has been used in this study by considering the effect of in-plane displacements u, v in addition to transverse and rotational displacements.

From this brief overview of the past literature, it is observed that a large body of research work has been carried out on the buckling characteristics of plates under uniform edge compression. On the contrary, relatively less amount of research works deal with the partial in-plane edge compression. Further, the buckling behaviour of isotropic stiffened plates under partial in-plane edge compression is sparsely treated in the literature. To the best knowledge of the authors, no comprehensive work is identified in the literature regarding in-plane partial edge load for stiffened laminated plates. The present work deals with the problem of vibration and buckling of stiffened composite laminates under the action of in-plane partial edge loads.

Analytical solution to this class of problems under such loadings is extremely difficult. Therefore, a nine-node heterosis element and a three node beam element are employed within the framework of finite element method. In this work, a detailed parametric study is carried out to investigate the effect of different ply-angles, boundary conditions, stiffener sizes, partial edge loads, and their positions on the vibration and stability behaviour of stiffened panels.

2 FORMULATION OF EQUATIONS WITH THEORY

The geometrical configuration of the bidirectional stiffened laminated plate of plan-form (a x b) with stiffeners parallel to x and y directions is shown in Figure 1. The middle-plane displacement fields corresponding to x, y, and z directions are u, v, and w, respectively.
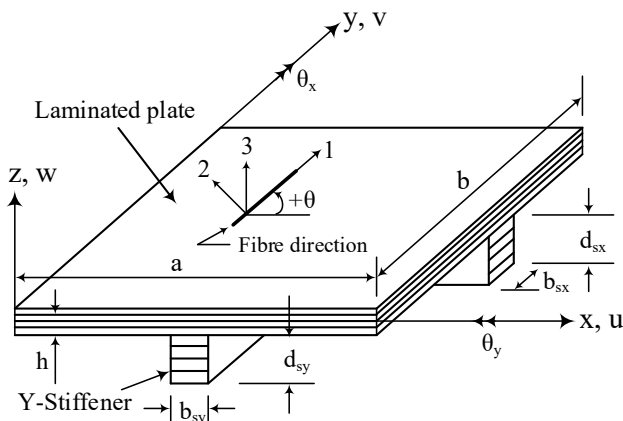

Figure 1: Laminate geometry of the plate with bidirectional stiffeners.

2.1 Strain-Displacement Relations

Lagrange's strain displacement equations are used throughout the formulation. The expressions pertaining to the linear strain relation of the plate by considering the effect of shear deformation are given by

$$\left. \begin{aligned}
\varepsilon_{xl} &= \frac{\partial u}{\partial x} + z\chi_x \\
\varepsilon_{yl} &= \frac{\partial v}{\partial y} + z\chi_y \\
\gamma_{xyl} &= \frac{\partial u}{\partial y} + \frac{\partial v}{\partial x} + z\chi_{xy} \\
\gamma_{xz} &= \frac{\partial w}{\partial x} + \theta_x \\
\gamma_{yz} &= \frac{\partial w}{\partial y} + \theta_y
\end{aligned} \right\} \tag{1}$$

where ε_{xl}, ε_{yl} and γ_{xyl} are the linear in-plane normal and shear strains; γ_{xz} and γ_{yz} are transverse shear strains; z is the distance of any layer from the middle plane of the plate and χ are the curvatures.

The expression for the non-linear strain displacement relation of the plate is as follows (Bathe, 1996)

$$\left.\begin{array}{rl}
\varepsilon_{xnl} &= \frac{1}{2}\left(\frac{\partial u}{\partial x}\right)^2 + \frac{1}{2}\left(\frac{\partial v}{\partial x}\right)^2 + \frac{1}{2}\left(\frac{\partial w}{\partial x}\right)^2 + \frac{1}{2}z^2\left[\left(\frac{\partial \theta_x}{\partial x}\right)^2 + \left(\frac{\partial \theta_y}{\partial x}\right)^2\right] \\[2ex]
\varepsilon_{ynl} &= \frac{1}{2}\left(\frac{\partial u}{\partial y}\right)^2 + \frac{1}{2}\left(\frac{\partial v}{\partial y}\right)^2 + \frac{1}{2}\left(\frac{\partial w}{\partial y}\right)^2 + \frac{1}{2}z^2\left[\left(\frac{\partial \theta_x}{\partial y}\right)^2 + \left(\frac{\partial \theta_y}{\partial y}\right)^2\right] \\[2ex]
\gamma_{xynl} &= \frac{\partial u}{\partial x}\frac{\partial u}{\partial y} + \frac{\partial v}{\partial x}\frac{\partial v}{\partial y} + \left(\frac{\partial w}{\partial x}\right)\left(\frac{\partial w}{\partial y}\right) + z^2\left[\frac{\partial \theta_x}{\partial x}\frac{\partial \theta_x}{\partial y} + \frac{\partial \theta_y}{\partial x}\frac{\partial \theta_y}{\partial y}\right]
\end{array}\right\} \quad (2)$$

where in, θ_x and θ_y are the rotations of normal to the un-deformed mid-plane of the plate about y and x axes, respectively.

The stress-strain relation for a lamina with reference to the plate axes is given by

$$\{\sigma\} = \left[\bar{Q}_{ij}\right]_k \{\varepsilon_l\} \quad (3)$$

By using Equations (1) and (3), the constitutive relation for the laminated plate can be given by

$$\begin{Bmatrix} \{N_i^p\} \\ \{M_i^p\} \\ \{Q_i^p\} \end{Bmatrix} = \begin{bmatrix} [A_{ij}^p] & [B_{ij}^p] & 0 \\ [B_{ij}^p] & [D_{ij}^p] & 0 \\ 0 & 0 & [S_{ij}^p] \end{bmatrix} \begin{Bmatrix} \{\varepsilon_j^p\} \\ \{\chi_j^p\} \\ \{\gamma_j^p\} \end{Bmatrix}$$

in short form,

$$\{N^P\} = \left[D^P\right]\{\varepsilon^P\} \quad (4)$$

where $\{N_i^P\} = \begin{bmatrix} N_x^P & N_y^P & N_{xy}^P \end{bmatrix}^T$ are stress resultants, $\{M_i^P\} = \begin{bmatrix} M_x^P & M_y^P & M_{xy}^P \end{bmatrix}^T$ are moment resultants, $\{Q_i^P\} = \begin{bmatrix} Q_{xz}^P & Q_{yz}^P \end{bmatrix}^T$ are transverse shear stress resultants; likewise, $\{\varepsilon_j^P\} = \begin{bmatrix} \varepsilon_x^P & \varepsilon_y^P & \gamma_{xy}^P \end{bmatrix}^T$ are the middle plane strains, $\{\chi_j^P\} = \begin{bmatrix} \chi_x^P & \chi_y^P & \chi_{xy}^P \end{bmatrix}^T$ are the middle plane curvatures and $\{\gamma_j^P\} = \begin{bmatrix} \gamma_{xz}^P & \gamma_{yz}^P \end{bmatrix}^T$ are the transverse shear strains. From Eq. (4), the extension-extension $\left[A_{ij}^P\right]$, extension-bending $\left[B_{ij}^P\right]$ and bending-bending $\left[D_{ij}^P\right]$ of the stiffness components can be expressed as

$$\left(A_{ij}^P,\ B_{ij}^P,\ D_{ij}^P\right) = \sum_{k=1}^{n}\int_{z_{k-1}}^{z_k}\left(\bar{Q}_{ij}\right)_k\left(1,\ z,\ z^2\right)dz, \quad i,\ j\ =\ 1,\ 2,\ 6 \quad (5)$$

and

$$S_{ij}^P = \sum_{k=1}^{n}\int_{z_{k-1}}^{z_k}\alpha\left(\bar{Q}_{ij}\right)_k dz, \quad i,\ j\ =\ 4,\ 5 \quad (6)$$

in which n is the number of layers, a is the shear correction factor, which is given by 5/6 (Kolli and Chandrashekhara, 1996; Reddy, 1996) and $\left[\bar{Q}_{ij}\right]_k$ is the stiffness matrix of kth lamina with reference to plate axes (Reddy, 1996).

The constitutive relationship for the laminated stiffeners can be written compactly as follows:

$$\{N^{sx}\} = [D^{sx}]\{\varepsilon^{sx}\} \tag{7}$$

$$\{N^{sy}\} = [D^{sy}]\{\varepsilon^{sy}\} \tag{8}$$

where $\{N^{sx}\} = [N_x^{sx} \ M_x^{sx} \ M_{xy}^{sx} \ Q_{xz}^{sx}]^T$ and $\{\varepsilon^{sx}\} = [\varepsilon_x^{sx} \ \chi_x^{sx} \ \chi_{xy}^{sx} \ \gamma_{xz}^{sx}]^T$ are the stress resultants and middle plane strains for the stiffener, respectively; $[D^{sx}]$ is the modified reduced constitutive matrix, which is obtained by ignoring the resultant stresses $(N_y^{sx} = N_{xy}^{sx} = M_y^{sx} = Q_{yz}^{sx} = 0)$ but not strains $(\varepsilon_y^{sx} \neq \gamma_{xy}^{sx} \neq \chi_y^{sx} \neq \gamma_{yz}^{sx} \neq 0)$ in the Eq. (4) and upon simplification, the reduced constitutive matrix of x-stiffener is obtained (Kolli and Chandrashekhara, 1996). A similar procedure is adopted to obtain the reduced constitutive matrix, $[D^{sy}]$ of y-stiffener.

2.2 Finite Element Formulation

In the present work, the plate has been discretized using nine-node (9-N) heterosis plate element with five degrees of freedom (DOF) given as u, v, w, θ_x and θ_y at all edge nodes and four DOF such as u, v, θ_x and θ_y at the inside node. The serendipity shape functions have been used for transverse DOF w, and Lagrange shape functions for remaining DOF that includes u, v, θ_x, θ_y as shown in Figure 2. In a discretization of stiffener, three-node beam element with four DOF at each node has been used viz., u, w, θ_x, θ_y for x-stiffener and v, w, θ_x, θ_y for y-stiffener. However, the other two kinds of quadratic elements such as eight-node (8-N) serendipity and nine-node (9-N) Lagrange elements have also been considered in this study as illustrated in Figure 2. The results of these quadratic elements are given only in comparison studies along with the results of heterosis element.
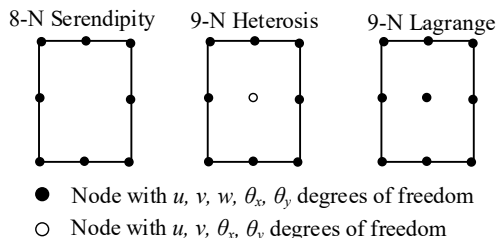
8-N Serendipity   9-N Heterosis   9-N Lagrange

● Node with u, v, w, θ_x, θ_y degrees of freedom
○ Node with u, v, θ_x, θ_y degrees of freedom

Figure 2: Different types of plate elements.

2.2.1 Elastic Stiffness Matrices

The total strain energy due to linear strains in the entire stiffened plate is given by

$$U_L = \frac{1}{2}\sum_{j=1}^{L}\int_v \{\varepsilon_l^p\}_j^T \{\sigma^p\}_j dv + \frac{1}{2}\sum_{j=1}^{L}\int_v \{\varepsilon_l^{sx}\}_j^T \{\sigma^{sx}\}_j dv + \frac{1}{2}\sum_{j=1}^{L}\int_v \{\varepsilon_l^{sy}\}_j^T \{\sigma^{sy}\}_j dv \tag{9}$$

where L is the number of elements of the plate or the x-stiffener or the y-stiffener involved in the formulation. After substituting Eqs (4), (7) and (8) in Eq. (9) and expressing linear strains,

$\{\varepsilon_l\} = [B]\{d_e\}$, in terms of derivatives of nodal shape functions and its corresponding displacement vectors, the linear part of the total strain energy can be obtained as,

$$
\begin{aligned}
U_L &= \frac{1}{2}\sum_{j=1}^{L}\{d_e\}^T\left[\left[k^p\right]+\left[k^{sx}\right]+\left[k^{sy}\right]\right]\{d_e\}, \\
&= \frac{1}{2}\{d\}^T\left[\left[K^p\right]+\left[K^{sx}\right]+\left[K^{sy}\right]\right]\{d\}, \\
&= \frac{1}{2}\{d\}^T\left[K\right]\{d\},
\end{aligned}
\tag{10}
$$

where $\{d_e\}$ and $\{d\}$ are the elemental and global displacement vectors, respectively; $\left[k^p\right]$, $\left[k^{sx}\right]$ and $\left[k^{sy}\right]$ are the element elastic stiffness matrices for plate, x-stiffener and y-stiffener, respectively; $\left[K\right]$ is the global stiffness matrix of the entire stiffened plate and are expressed as,

$$
\left[k^p\right] = \int_{-1}^{+1}\int_{-1}^{+1}[B^p]^T[D^p][B^p]\left|J_p\right|d\xi d\eta,
\tag{11}
$$

$$
\left[k^{sx}\right] = \int_{-1}^{+}[E^{sx}]^T[B^{sx}]^T[D^{sx}][B^{sx}][E^{sx}]\left|J_{sx}\right|d\xi,
\tag{12}
$$

$$
\left[k^{sy}\right] = \int_{-1}^{+}[E^{sy}]^T[B^{sy}]^T[D^{sy}][B^{sy}][E^{sy}]\left|J_{sy}\right|d\eta,
\tag{13}
$$

where $\left[E^{sx}\right]$ and $\left[E^{sy}\right]$ are the transformation matrices; $\left[B^p\right]$, $\left[B^{sx}\right]$ and $\left[B^{sy}\right]$ are the elemental strain displacement matrices for plate, x-stiffener and y-stiffener, respectively, wherein

$$
[B^P] = \left[\begin{array}{ccccc}
\dfrac{\partial N_i}{\partial x} & 0 & 0 & 0 & 0 \\
0 & \dfrac{\partial N_i}{\partial y} & 0 & 0 & 0 \\
\dfrac{\partial N_i}{\partial y} & \dfrac{\partial N_i}{\partial x} & 0 & 0 & 0 \\
0 & 0 & 0 & \dfrac{\partial N_i}{\partial x} & 0 \\
0 & 0 & 0 & 0 & \dfrac{\partial N_i}{\partial y} \\
0 & 0 & 0 & \dfrac{\partial N_i}{\partial y} & \dfrac{\partial N_i}{\partial x} \\
0 & 0 & \dfrac{\partial N_i}{\partial x} & N_i & 0 \\
0 & 0 & \dfrac{\partial N_i}{\partial y} & 0 & N_i
\end{array}\right|_{i=1,2..8}
\left.\begin{array}{cccc}
\dfrac{\partial N_9}{\partial x} & 0 & 0 & 0 \\
0 & \dfrac{\partial N_9}{\partial y} & 0 & 0 \\
\dfrac{\partial N_9}{\partial y} & \dfrac{\partial N_9}{\partial x} & 0 & 0 \\
0 & 0 & \dfrac{\partial N_9}{\partial x} & 0 \\
0 & 0 & 0 & \dfrac{\partial N_9}{\partial y} \\
0 & 0 & \dfrac{\partial N_9}{\partial y} & \dfrac{\partial N_9}{\partial x} \\
0 & 0 & N_9 & 0 \\
0 & 0 & 0 & N_9
\end{array}\right]
\tag{14}
$$

and

$$
[B^{sx}] = \begin{bmatrix} \dfrac{\partial N_i^{sx}}{\partial x} & 0 & 0 & 0 \\[2mm] 0 & 0 & \dfrac{\partial N_i^{sx}}{\partial x} & 0 \\[2mm] 0 & 0 & 0 & \dfrac{\partial N_i^{sx}}{\partial x} \\[2mm] 0 & \dfrac{\partial N_i^{sx}}{\partial x} & N_i^{sx} & 0 \end{bmatrix}; \quad [B^{sy}] = \begin{bmatrix} \dfrac{\partial N_i^{sy}}{\partial y} & 0 & 0 & 0 \\[2mm] 0 & 0 & 0 & \dfrac{\partial N_i^{sy}}{\partial y} \\[2mm] 0 & 0 & \dfrac{\partial N_i^{sy}}{\partial y} & 0 \\[2mm] 0 & \dfrac{\partial N_i^{sy}}{\partial y} & 0 & N_i^{sy} \end{bmatrix}_{i=1,3} \tag{15}
$$

and also

$$
[E^{sx}] = \sum_{i=1}^{3} \begin{bmatrix} 1 & 0 & 0 & e_{sx} & 0 \\ 0 & 0 & 1 & 0 & 0 \\ 0 & 0 & 0 & 1 & 0 \\ 0 & 0 & 0 & 0 & 1 \end{bmatrix}; \quad [E^{sy}] = \sum_{i=1}^{3} \begin{bmatrix} 0 & 1 & 0 & 0 & e_{sy} \\ 0 & 0 & 1 & 0 & 0 \\ 0 & 0 & 0 & 1 & 0 \\ 0 & 0 & 0 & 0 & 1 \end{bmatrix} \tag{16}
$$

in which $e_{sx} = (d_{sx} + h)/2$ and $e_{sy} = (d_{sy} + h)/2$ are stiffener eccentricities.

2.2.2 Geometric Stiffness Matrices

The total strain energy due to non-linear strains in the entire stiffened plate is given by

$$
U_L = \frac{1}{2} \sum_{j=1}^{L} \int_v \{\varepsilon_l^p\}_j^T \{\sigma^p\}_j dv + \frac{1}{2} \sum_{j=1}^{L} \int_v \{\varepsilon_l^{sx}\}_j^T \{\sigma^{sx}\}_j dv + \frac{1}{2} \sum_{j=1}^{L} \int_v \{\varepsilon_l^{sy}\}_j^T \{\sigma^{sy}\}_j dv \tag{17}
$$

Substituting the non-linear strain displacement of plate [Eq. (2)] and the corresponding stiffeners in the above equation and upon simplification, we get the final form of Eq. (17) as given below:

$$
\begin{aligned}
U_{NL} &= \frac{1}{2} \sum_{j=1}^{L} \{d_e\}^T \left[[k_G^p] + [k_G^{sx}] + [k_G^{sy}] \right] \{d_e\}, \\
&= \frac{1}{2} \{d\}^T \left[[K_G^p] + [K_G^{sx}] + [K_G^{sy}] \right] \{d\}, \\
&= \frac{1}{2} \{d\}^T [K_G] \{d\},
\end{aligned} \tag{18}
$$

where $[k_G^p]$, $[k_G^{sx}]$ and $[k_G^{sy}]$ are the elemental geometric stiffness matrices for plate, x-stiffener and y-stiffener, respectively; $[K_G]$ is the overall geometric stiffness matrix of the entire stiffened plate, which are expressed as,

$$
[k_G^p] = \int_{-1}^{+1} \int_{-1}^{+1} [B_G^p]^T [S^p][B_G^p] |J_p| d\xi d\eta, \tag{19}
$$

$$
[k_G^{sx}] = \int_{-1}^{+} [E^{sx}]^T [B_G^{sx}]^T [S^{sx}][B_G^{sx}][E^{sx}] |J_{sx}| d\xi, \tag{20}
$$

$$[k_G^{sy}] = \int_{-1}^{+} [E^{sy}]^T [B_G^{sy}]^T [S^{sy}][B_G^{sy}][E^{sy}]|J_{sy}| d\eta, \qquad (21)$$

where $[B_G^P]$, $[B_G^{sx}]$ and $[B_G^{sy}]$ are the elemental non-linear strain displacement matrices for plate, x-stiffener and y-stiffener, respectively; $[S^P]$, $[S^{sx}]$ and $[S^{sy}]$ are the corresponding initial pre-buckling stress matrices, in which

$$[B_G^P] = \begin{bmatrix} \dfrac{\partial N_i}{\partial x} & 0 & 0 & 0 & 0 & \dfrac{\partial N_9}{\partial x} & 0 & 0 & 0 \\ \dfrac{\partial N_i}{\partial y} & 0 & 0 & 0 & 0 & \dfrac{\partial N_9}{\partial y} & 0 & 0 & 0 \\ 0 & \dfrac{\partial N_i}{\partial x} & 0 & 0 & 0 & 0 & \dfrac{\partial N_9}{\partial x} & 0 & 0 \\ 0 & \dfrac{\partial N_i}{\partial y} & 0 & 0 & 0 & 0 & \dfrac{\partial N_9}{\partial y} & 0 & 0 \\ 0 & 0 & \dfrac{\partial N_i}{\partial x} & 0 & 0 & 0 & 0 & 0 & 0 \\ 0 & 0 & \dfrac{\partial N_i}{\partial y} & 0 & 0 & 0 & 0 & 0 & 0 \\ 0 & 0 & 0 & \dfrac{\partial N_i}{\partial x} & 0 & 0 & 0 & \dfrac{\partial N_9}{\partial x} & 0 \\ 0 & 0 & 0 & \dfrac{\partial N_i}{\partial y} & 0 & 0 & 0 & \dfrac{\partial N_9}{\partial y} & 0 \\ 0 & 0 & 0 & 0 & \dfrac{\partial N_i}{\partial x} & 0 & 0 & 0 & \dfrac{\partial N_9}{\partial x} \\ 0 & 0 & 0 & 0 & \dfrac{\partial N_i}{\partial y} & 0 & 0 & 0 & \dfrac{\partial N_9}{\partial y} \end{bmatrix}_{i=1,2..8} \qquad (22)$$

and

$$[B_G^{sx}] = \begin{bmatrix} \dfrac{\partial N_i^{sx}}{\partial x} & 0 & 0 & 0 \\ 0 & \dfrac{\partial N_i^{sx}}{\partial x} & 0 & 0 \\ 0 & 0 & \dfrac{\partial N_i^{sx}}{\partial x} & 0 \\ 0 & 0 & 0 & \dfrac{\partial N_i^{sx}}{\partial x} \end{bmatrix}_{i=1,3} \qquad (23)$$

and

$$[S^{sx}] = \begin{bmatrix} [s^{sx}]_1 & 0 & 0 & 0 \\ 0 & [s^{sx}]_1 & 0 & 0 \\ 0 & 0 & [s^{sx}]_2 & 0 \\ 0 & 0 & 0 & [s^{sx}]_2 \end{bmatrix} \qquad (24)$$

in which

$$[S^{sx}]_1 = d_{sx}\sigma^{0sx} = N^{0sx} \tag{25}$$

$$[S^{sx}]_2 = \frac{d_{sx}^3}{12}\sigma^{0sx} = \frac{d_{sx}^2}{12}N^{0sx} \tag{26}$$

2.2.3 Consistent Mass Matrices

The abbreviated form of total kinetic energy in the entire stiffened plate by including the effect of in-plane inertia, transverse inertia and rotational inertia is as follows:

$$
\begin{aligned}
T &= \frac{1}{2}\sum_{j=1}^{L}\left\{\dot{d}_e\right\}^T\left[[m^p]+[m^{sx}]+[m^{sy}]\right]\left\{\dot{d}_e\right\}, \\
&= \frac{1}{2}\left\{\dot{d}\right\}^T\left[[M^p]+[M^{sx}]+[M^{sy}]\right]\left\{\dot{d}\right\}, \\
&= \frac{1}{2}\left\{\dot{d}\right\}^T[M]\left\{\dot{d}\right\},
\end{aligned}
\tag{27}
$$

where as $[m^P]$, $[m^{sx}]$ and $[m^{sy}]$ are the elemental mass matrices for plate, x-stiffener and y-stiffener, respectively; $[M]$ is the overall mass matrix of the entire stiffened plate, which are expressed as,

$$[m^p] = \int_{-1}^{+1}\int_{-1}^{+1}[\bar{N}^p]^T[\bar{I}^p][\bar{N}^p]|J_p|d\xi d\eta, \tag{28}$$

$$[m^{sx}] = \int_{-1}^{+}[E^{sx}]^T[\bar{N}^{sx}]^T[\bar{I}^{sx}][\bar{N}^{sx}][E^{sx}]|J_{sx}|d\xi, \tag{29}$$

$$[m^{sy}] = \int_{-1}^{+}[E^{sy}]^T[\bar{N}^{sy}]^T[\bar{I}^{sy}][\bar{N}^{sy}][E^{sy}]|J_{sy}|d\eta, \tag{30}$$

in which

$$
[\bar{I}^p] = \begin{bmatrix}
\bar{I}_1 & 0 & 0 & \bar{I}_2 & 0 \\
0 & \bar{I}_1 & 0 & 0 & \bar{I}_2 \\
0 & 0 & \bar{I}_1 & 0 & 0 \\
\bar{I}_2 & 0 & 0 & \bar{I}_3 & 0 \\
0 & \bar{I}_2 & 0 & 0 & \bar{I}_3
\end{bmatrix}
\tag{31}
$$

and

$$\left[\overline{I}^{sx}\right] = \begin{bmatrix} \overline{I}_1 & 0 & \overline{I}_2 & 0 \\ 0 & \overline{I}_1 & 0 & 0 \\ \overline{I}_2 & 0 & \overline{I}_3 & 0 \\ 0 & 0 & 0 & \overline{I}_3 \end{bmatrix} \tag{32}$$

with

$$\left(\overline{I}_1, \overline{I}_2, \overline{I}_3\right) = \sum_{k=1}^{L} \int_{z_{k-1}}^{z_k} \rho_k \left(1, z, z^2\right) dz. \tag{33}$$

2.3 Governing Equations

The governing equation of motion for vibration and stability problems derived using extended Hamilton's principle is given below:

$$\Delta \int_{t_1}^{t_2} (T - U) dt = \{0\}. \tag{34}$$

where T is the kinetic energy for entire stiffened plate, U is the strain energy due to linear and nonlinear strains; t_1, t_2 are two arbitrary values of time t and Δ denotes the variational operator.

Substituting Eqns (10), (18) and (27) into the Eq. (34) and upon simplification, the following most general governing differential equation of motion is obtained as follows:

$$[M]\{\ddot{q}\} + [K]\{q\} - P[K_G]\{q\} = \{0\}. \tag{35}$$

The governing equations for the vibration and buckling can be obtained separately by reducing Eq. (35) as follows:

Vibration problem: When the stiffened/unstiffened plate vibrates harmonically with a given in-plane load, Eq. (35) reduces to

$$\left[[K] - P[K_G]\right]\{q\} - \omega^2 [M]\{q\} = \{0\}. \tag{36}$$

Buckling problem: when $\{\ddot{q}\} = \{0\}$, Eq. (35) reduces to

$$[K]\{q\} - P_{cr}[K_G]\{q\} = \{0\}, \tag{37}$$

where P_{cr} is the critical load and P is the applied edge compression.

Both Eqs (36) and (37) represent the eigenvalue problems. The square of frequency, ω^2, for an applied in-plane load P is the eigenvalue in Eq. (36) and the critical load P_{cr} is the eigenvalue in Eq. (37).

Eigenvector $\{q\}$ represents the corresponding mode shapes of vibration or buckling problems.

3 NUMERICAL RESULTS AND DISCUSSIONS

3.1 Computer Program

The solution of stability problems using either dynamic or static approach involves extraction of eigenvalues and eigenvectors, as evidenced in Eqs (36) and (37) respectively. The large sized matrices appearing in these two equations have to be stored in skyline form. Bathe (1996) has given the time-tested code in FORTRAN for extraction of the eigenvalues using the subspace iteration technique. To be compatible with this, the FORTRAN code has been developed to generate various element level and global matrices and finally stored these matrices in skyline assembled form.

In the code, a selective integration scheme is incorporated for the generation of element elastic stiffness matrix. A 3 x 3 Gauss rule is adopted for membrane as well as bending effects while 2 x 2 Gauss rule is adopted for shear effects. As the geometric stiffness matrix is a function of the pre-buckling stress field in an element due to the application of any kind of in-plane loads, it is a prerequisite to perform the plane stress analysis before the generation of geometric stiffness matrix. Hence, code is done for the plane stress analysis to evaluate the stress field at 3 x 3 Gauss points. Accordingly, the integration for the generation of geometric stiffness matrix has been done using 3 x 3 Gauss rule (full integration). Similarly, A 3 x 3 Gauss rule is adopted to evaluate element level mass matrix also.

3.2 Boundary Conditions, Stiffener Parameters and Material Constants

In the present work, for the configuration of the stiffened laminated plate shown in Figure 1, two types of boundary conditions have been employed are as follows:

(1) Simply supported (S-S-S-S):
  (i)   for initial pre-buckled stress analysis: along the edges (a) $x = 0$, a; $w = \theta_y = 0$, (b) $y = 0$, b; $w = \theta_x = 0$ and at $x = a/2$, $u = 0$; at $y = b/2$, $v = 0$
  (ii) for buckling analysis: along the edges (a) $x = 0$, a; $u = w = \theta_y = 0$, (b) $y = 0$, b; $v = w = \theta_x = 0$.
(2) Clamped supported (C-C-C-C):
  (iii) for initial pre-buckled stress analysis: along the edges (a) $x = 0$, a; $w = \theta_x = \theta_y = 0$, (b) $y = 0$, b; $w = \theta_x = \theta_y = 0$ and at $x = a/2$, $u = 0$; at $y = b/2$, $v = 0$
  (i)   for buckling analysis: along the edges (a) $x = 0$, a; $u = v = w = \theta_x = \theta_y = 0$, (b) $y = 0$, b; $u = v = w = \theta_x = \theta_y = 0$.

The stiffener dimensions are decided according to the non-dimensional parameters, in which δ and β are defined as: $\delta = nA_s/bh$ which is the ratio of total area of the stiffeners to that of the plate, where n is the number of stiffeners and A_s is the cross-sectional area of each stiffener; similarly, $\beta = nE_2I_s/bD$ is the ratio of total bending stiffness of the stiffeners to that of the plate, where I_s is the moment of inertia of the stiffener about the plate centroidal axis and D is the flexural rigidity of the plate, which is $D = Eh^3/12(1 - \upsilon^2)$ for isotropic case and $D = E_2h^3/12(1 - \upsilon_{12}^2)$ for composite case. The ratio of thickness of plate to the width of the plate (h/b) is considered as 0.01 unless otherwise stated.

The vibration frequency and the critical loads are represented in non-dimensional form as given in Table 1 and the elastic material properties with reference to the principal axes have been given in Table 2 unless otherwise mentioned.

Parameters	Stiffened/unstiffened plates	
	Isotropic	Composite
Natural frequencies(ϖ)	$\omega b^2 \sqrt{\rho h / D}$	$\omega b^2 \sqrt{\rho h / E_2 h^2}$
Buckling load (γ_{cr})	$P_{cr} b^2 / D$	$P_{cr} b^2 / E_2 h^3$

Table 1: Non-dimensional parameters (Deolasi et al., 1995; Leissa and Ayoub, 1988; Reddy and Phan, 1985).

In Table 1, ω is the absolute value of frequency, ρ is the material density, D is the flexural rigidity of the plate and P_{cr} is the absolute critical buckling load.

Material	Stiffened/unstiffened plates					
	E_{11}	E_{22}	G_{12}	G_{13}	G_{23}	ν_{12}
Isotropic	1.0	1.0	0.3854	0.3854	0.3854	0.30
Composite	25.0	1.0	0.50	0.50	0.20	0.25

Table 2: Material constants (Reddy, 1996; Sundaresan et al., 1998; Xiao et al., 2008).

3.3 Comparative Studies

The validation of the finite element formulation described above is necessary to ascertain the correctness of the development of various matrices involved in the analysis of vibration and buckling problems. From the comparative studies of deflections and rotations for unstiffened/stiffened plates subjected to lateral loads, one can ascertain the validity of the elastic stiffness matrix. After ascertaining this, if the vibration frequencies are compared, the formulation of the mass matrix can be validated. Finally, if the buckling loads are compared with the classical/numerical solutions, the generation of the geometric stiffness matrix can be validated. Validation of all these matrices has been carried out as described in the following sub-sections.

3.3.1 Static Analysis of Laminated Stiffened and Unstiffened Plates

The values of deflection of unstiffened/stiffened laminated plates under lateral loads are determined and the results are represented in Table 3 and Table 4, respectively. The effect of uniformly distributed load $(\bar{q})$ on the central deflection $(\bar{W})$ of a laminated plate is tabulated in Table 3 along with the results of Reddy (1996) and 3D-FEM solutions (Xiao et al., 2008). The results show very good agreement with the analytical solution. Table 4 shows the central deflection of a laminated square plate with centrally placed bidirectional stiffeners subjected to various boundary conditions with the material properties pertaining to AS4/3501 graphite/epoxy composite: $E_{11} = 144.8$ GPa; $E_{22} = 9.65$ GPa; $G_{12} = G_{13} = 4.14$ GPa; $G_{23} = 3.45$ GPa; $\nu_{12} = 0.3$; $\rho = 1389.23$ kg/m^3. Similarly, the geomet-

rical dimensions of the stiffened plate [see Figure 1] are as follows: $a = 254$ mm, $b = 254$ mm, $h = 12.7$ mm, $b_{sx} = b_{sy} = 6.35$ mm and $d_{sx} = d_{sy} = 25.4$ mm. The results using nine-node heterosis element and eight-node serendipity element are depicted in Table 4. It can be observed that both the elements give satisfactory results. However, the results of heterosis element seem to be more accurate when compared to those obtained from eight-node element and nine-node element, which was previously used by Kolli and Chandrashekhara (1996). The satisfactory agreement of the results with the literature clearly shows the correctness in the formulation of element elastic stiffness matrix for both plate $\left[k^{P} \right]$ as well as stiffeners $\left[k^{sx} \right]$ and $\left[k^{sy} \right]$.

Source	b/h	0	0/90/0	0/90/90/0	0/90/0/90/0	$((0/90/90)\,\overline{0}\,)_2$
Closed-form (Reddy, 1996)		0.952	1.022	1.025	0.973	0.964
3D-FEM(Xiao et al., 2008)	10	0.948	1.154	1.140	1.058	--
Present (heterosis)		0.952	1.022	1.025	0.973	0.957
Closed-form (Reddy, 1996)		0.726	0.757	0.769	0.758	0.758
3D-FEM(Xiao et al., 2008)	20	0.726	0.795	0.803	0.779	--
Present (heterosis)		0.726	0.757	0.769	0.758	0.756
Closed-form (Reddy, 1996)	100	0.653	0.670	0.683	0.687	0.690
Present (heterosis)		0.653	0.670	0.683	0.687	0.690

Table 3: Non-dimensionalised central deflection $\overline{w} = (w_{max} E_2 h^3 / \overline{q} a^4)\,10^2$ for different cross-ply laminated simply supported unstiffened square plate.

	Distributed load ($\overline{q} = 0.6895$ N/mm^2)				Point load ($q_0 = 4.448$ KN)			
B.C	[0/90]		[45/-45]		[0/90]		[45/-45]	
	Present	Kolli et al. (1996)	Present	Kolli et al. (1996)	Present	Kolli et al. (1996)	Present	Kolli et al. (1996)
S-S-S-S	(0.9094) (0.9058)	0.9118	(1.3125) (1.3143)	1.3117	(0.2836) (0.2778)	0.2890	(0.3839) (0.3807)	0.3879
C-C-C-C	(0.3666) (0.3506)	0.3700	(0.4411) (0.4317)	0.4415	(0.1619 (0.1529)	0.1675	(0.1931) (0.1876)	0.1973
S-S-C-C	(0.5717) (0.5597)	0.5748	(0.6844) (0.6818)	0.6850	(0.2119) (0.2038)	0.2175	(0.2478) (0.2439)	0.2520

Note: Values within the first parentheses indicate the result from nine-node heterosis element and those in second parentheses from eight-node serendipity element.

Table 4: Central deflection of a laminated plate with centrally placed bidirectional stiffeners.

3.3.2 Vibration Study of Laminated Unstiffened and Stiffened Plates

To further validate the formulation of the mass matrix, the free vibration characteristics of an unstiffened square composite plate are studied using nine-node heterosis element (9-NHE); the results are presented in Table 5 along with the closed-form solutions (CFS) given by Reddy and Phan (1985). However, to ascertain the performance of other kinds of elements, the authors have also studied the free vibration behaviour using nine-node Lagrange element (9-NLE) and eight-node serendipity element (8-NSE). It is concluded that the adoption of nine node heterosis element in the formulation is a better choice than the use of other elements.

	2 layers (45/-45)				8 layers (45/-45/45...)			
b/h	Present results			CFS (Reddy and Phan, 1985)	Present results			CFS (Reddy and Phan, 1985)
	9-NHE	9-NLE	8-NSE		9-NHE	9-NLE	8-NSE	
5	10.335	10.244	10.243	10.335	12.892	12.863	12.862	12.892
10	13.044	12.975	12.975	13.044	19.289	19.235	19.235	19.289
20	14.179	14.154	14.153	14.179	23.259	23.225	23.225	23.259
25	14.338	14.322	14.321	14.338	23.924	23.899	23.899	23.924
50	14.561	14.557	14.556	14.561	24.909	24.902	24.901	24.909
100	14.618	14.617	14.617	14.618	25.176	25.174	25.174	25.176

Table 5: Non-dimensionalised frequency of an angle-ply laminated simply supported unstiffened square plate; $E_{11}/E_{22} = 40$, $G_{12} = G_{13} = 0.6E_{22}$, $G_{23} = 0.5E_{22}$, $v_{12} = 0.25$.

		0/90				45/-45		
B.C	Mode no.	Satish Kumar and Mukhopadhyay (2000)	Thinh and Khoa (2008)	Thinh and Quoc (2008)	Present (heterosis element)	Satish Kumar and Mukhopadhyay (2000)	Thinh and Khoa (2008)	Present (heterosis element)
S-S-S-S	1	1076.0	1014.0	1053.6	1030.1	1005.7	1007.1	980.9
	2	2059.6	2139.5	2083.7	2221.3	2254.4	2284.7	2343.3
	3	2302.7	2397.9	2327.6	2446.3	2358.7	2434.5	2352.9
	4	2635.8	2683.0	2556.9	2689.1	3247.4	3208.3	3293.6
C-C-C-C	1	1666.5	1542.1	1609.5	1783.4	1714.2	1573.8	1662.5
	2	2929.2	2848.3	2926.3	3070.8	3049.3	2909.4	3043.6
	3	3140.1	3041.4	3141.2	3253.8	3077.4	2967.7	3048.6
	4	3666.3	3653.5	3639.2	3665.6	3943.9	3896.3	3948.5
C-C-S-S	1	1445.8	1333.7	1427.5	1453.9	1380.9	1304.0	1340.9
	2	2107.7	2259.6	2083.9	2441.8	2471.6	2483.6	2485.7
	3	3054.0	2929.5	2896.7	3042.2	2912.6	2835.2	2914.3
	4	3196.8	3221.7	3209.9	3232.6	3609.6	3557.0	3635.1

Table 6: Comparison of absolute natural frequencies of a laminated plate with bidirectional stiffeners.

Similar to the comparative analysis carried out for an unstiffened plate, the studies are further extended to a laminated plate with centrally placed bidirectional stiffeners under various edge conditions and the results are tabulated in Table 6 along with those available in the literature (Satish Kumar and Mukhopadhyay, 2000; Thinh and Khoa, 2008; Thinh and Quoc, 2008). The geometric and material properties of the stiffened plate are similar to the case 3.3.1. The comparison of results establishes the correctness of the mass matrix formulation for both the plate as well as the stiffeners.

3.3.3 Buckling Characteristics of Unstiffened/Stiffened Plates

For the buckling analysis, as in Eqs 36 and 37, one more matrix called geometric stiffness matrix appears in the formulation of the problem. It is essential to validate the formulation of such matrix. In this regard, a non-dimensional quantity η (load bandwidth ratio) is introduced, which is either the ratio of the position of the concentrated load to the width of the plate or width of edge compression to the width of the plate [refer Figures 3, 5 and 6]. The critical loads for an unstiffened plate under concentrated load [see Figure 3(a)] are found for $\eta = 0.25$ and 0.5 and compared in Table 7 with those available in the literature (Deolasi et al., 1995; Leissa and Ayoub, 1988). Similarly, a comparative study has been carried out for an S-S-S-S edged laminated plate with partial in-plane load [see Figure 3 (b)] for various η and ply-orientations as shown in Figure 4. The non-dimensionalised critical loads are validated with the results given by Sundaresan et al. (1998). It is to be noted here that γ is the critical load for a fully loaded plate and γ_{cr} is the critical load for a partially loaded plate.

Further, the buckling behaviour of S-S-S-S edged plate with a central single stiffener under uniformly distributed edge load over width b is studied for different bending rigidity of the stiffener. The value of δ is varied from 0.05 to 0.20, and that of β from 5 to 15. The results are presented in Table 8 in non-dimensionalised form as $\gamma_{cr} = P_{cr} b^2 /(\pi^2 D)$, and compared with the classical solution of Timoshenko and Gere (1961), numerical solutions of Mukhopadhyay and Mukherjee (1990), and Hamedani and Ranji (2013). In all the cases, the present results agree well with those available in the literature confirming the correctness of the geometric stiffness matrix for the plate as well as the stiffeners.
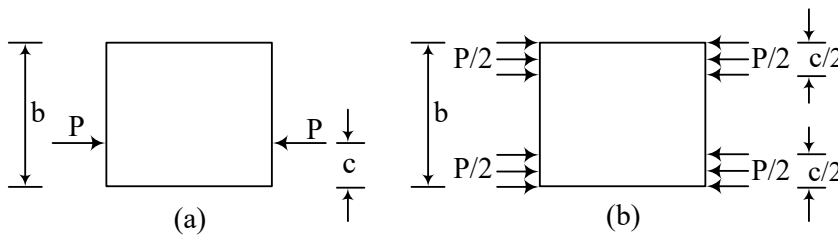

Figure 3: Unstiffened plate under (a) Concentrated edge load from one edge; (b) Partial edge load from both edges.

a/b	η	Leissa and Ayoub (1988)	Deolasi et al. (1995)	Present
0.5	0.25	38.282	37.608	37.249
	0.50	30.061	29.852	29.630
1.0	0.25	37.000	36.405	36.316
	0.50	25.814	25.720	25.658
2.0	0.25	36.954	36.832	36.659
	0.50	26.523	28.851	28.690

Table 7: Non-dimensionalised critical loads γ_{cr} for S-S-S-S edged isotropic
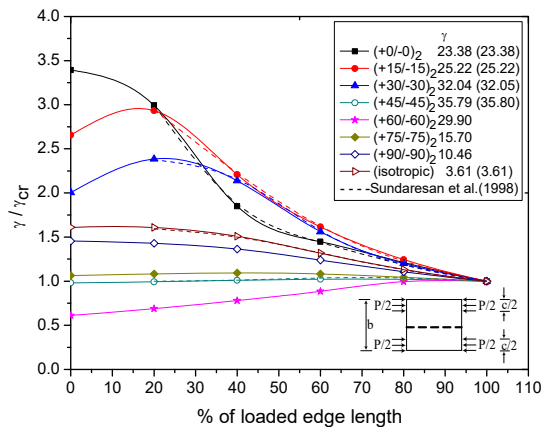plate under concentrated load [Figure 3 (a)].

Figure 4: Comparison of γ / γ_{cr} with % of edge load length for various angle-plies unstiffened
square plate with uniaxial partial in-plane loading from both the edges [Figure 3 (b)].

β	δ	Non-dimensional buckling load					
		Neglecting T and e				Considering T and e	
		Timoshenko and Gere (1961)	Mukhopadhyay and Mukherjee (1990)	Jafarpour and Ranji (2013)	Present (heterosis)	Jafarpour and Ranji (2013)	Present (heterosis)
	0.05	12.00	11.72	11.89	11.80	11.91	11.86
5	0.10	11.10	10.93	11.08	10.98	11.09	11.27
	0.20	9.72	9.70	9.85	9.69	9.86	10.01
	0.05	16.00	16.00	16.01	15.97	18.16	17.91
10	0.10	16.00	16.00	16.01	15.97	16.97	17.20
	0.20	15.80	15.44	15.01	15.67	15.04	15.77
	0.05	16.00	16.00	16.01	15.97	20.41	20.30
15	0.10	16.00	16.00	16.01	15.97	20.41	20.33
	0.20	16.00	16.00	16.01	15.97	19.36	20.33

T and e = Torsional rigidity and eccentricity of the stiffener

Table 8: Validation of non-dimensional critical loads for a simply supported square stiffened plate.

3.4 Convergence Study

In the finite element method, it is essential to appropriately discretize the structure for proper convergence of results. In this regard, the plate is discretized into m, number of rows and n, number of columns, i.e. m x n plate elements as shown in Figure 5. Table 9 shows the convergence of the non-dimensional critical loads for an unstiffened/stiffened plate under the action of uniaxial compressive edge load from one edge. The Table 9 also shows the non-dimensional vibration frequencies under the action of in-plane edge loads $P/P_{cr} = +0.5$ (compressive) and $P/P_{cr} = 0$ (no in-plane load). It is observed that the convergence of results is satisfactory for the mesh size of 10 x 10 and hence this mesh size is maintained throughout the work.
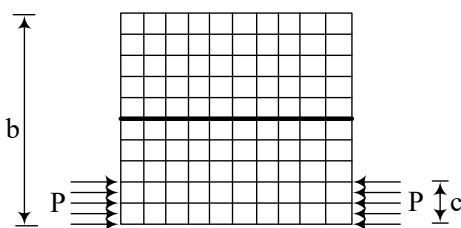
Figure 5: Laminated plate with centrally placed single stiffener along x-axis and load from one edge.

η	Mesh order m x n	Un-stiffened plate			Stiffened plate		
		Buckling load (γ_{cr})	[P/Pcr] frequency (ϖ)		Buckling load (γ_{cr})	[P/Pcr] frequency (ϖ)	
			0	0.5		0	0.5
0.5	4 x 4	28.68	17.80	12.91	68.39	29.35	22.03
	6 x 6	28.55	17.78	12.90	67.11	29.16	21.89
	8 x 8	28.54	17.78	12.90	66.84	29.12	21.87
	10 x 10	28.53	17.78	12.90	66.76	29.12	21.87
	12 x 12	28.53	17.78	12.90	66.75	29.12	21.87
1.0	4 x 4	32.10	17.80	12.59	97.59	29.35	20.78
	6 x 6	32.06	17.78	12.57	97.19	29.16	20.64
	8 x 8	32.05	17.78	12.57	95.96	29.12	20.62
	10 x 10	32.04	17.78	12.57	95.90	29.12	20.61
	12 x 12	32.04	17.78	12.57	95.89	29.12	20.61

Table 9: Convergence of buckling load (γ_{cr}) and frequency parameters (ϖ) for an S-S-S-S edged angle-ply $(+30°/-30°)_2$ square plate with/without central stiffener ($\delta = 0.1$ and $\beta = 10$).

3.5 Vibration and Buckling Behaviour of Laminated Stiffened Plate under Variety of Partial Edge Loading

In the present study, the buckling and vibration characteristics of a plate with centrally placed stiffener/s subjected to uni-/bidirectional partial in-plane compressive loads have been investigated. Figure 6 shows the configuration of the stiffened plates with different kinds of in-plane edge loads.

For buckling analysis, an initial pre-buckling stress field has to be determined where the total load, P acting on the plate is constant irrespective of the type and width of loading. Also, the total volume of stiffened plate is same irrespective of the number of stiffeners in any directions.
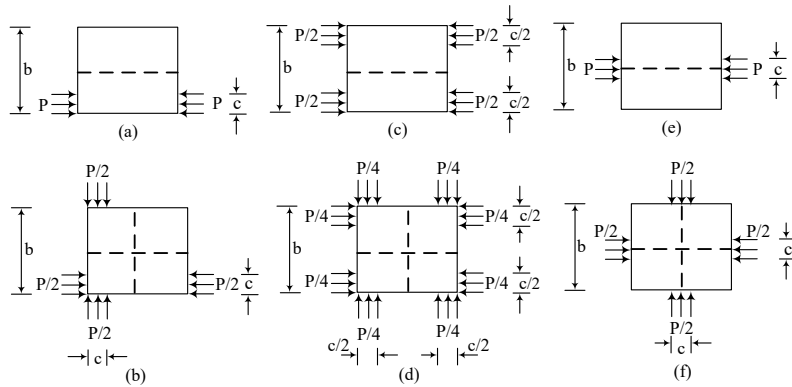

Figure 6: Simply supported/clamped stiffened plates subjected to various loading cases:
(a) Partial edge load from one edge; (b) Partial edge load from two adjacent edges;
(c) Partial edge load from two opposite edges; (d) Partial edge load from all the corners;
(e) Partial edge load from the center, unidirectional; (f) Partial edge load from the center, bidirectional.

3.5.1 Vibration Characteristics of Laminated Stiffened Plate under Uniaxial Edge Loading

The effect of non-dimensional load λ on the vibration behaviour of S-S-S-S edged laminated square plate with a centrally placed single stiffener has been studied for $\delta = 0.1$ and $\beta = 10$. This load case is shown in Figure 6 (a). The results presented in Figures 7 (a) and (b) indicate that the frequency decreases with an increase in the value of edge load. As the load approaches the critical value, the vibration frequency reduces to zero and this load is called the buckling load. This dynamic method of analysis overcomes the shortcomings of the evaluation of critical loads by the static approach, which generally happens where the in-plane stress distribution within an element is significantly non-uniform. This method of analysis has been adopted to determine the critical loads for various problems discussed henceforth.
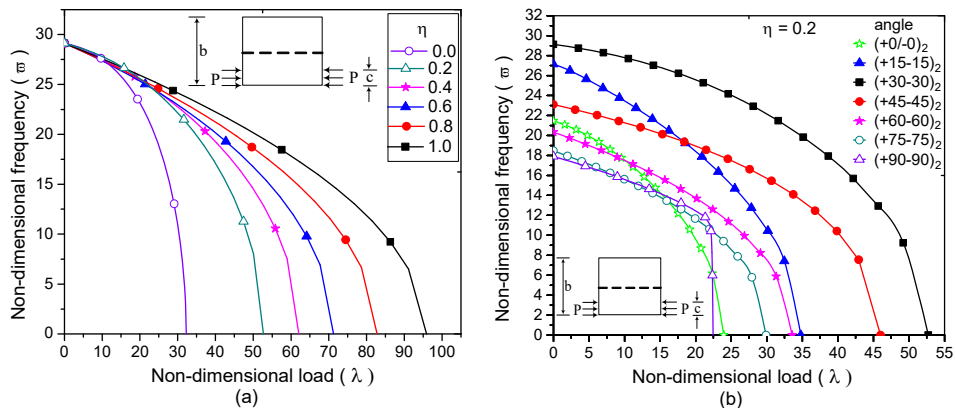
Figure 7: Variation of frequency parameter (ϖ) vs non-dimensional load λ (a) for a ply-orientation of $(\pm 30^{\circ})_2$ with different values of η (b) for $\eta = 0.2$ with different ply-orientations.

3.5.2 Laminated Stiffened Plate under Uniaxial and Biaxial Partial Edge Load from One Edge

The effect of a four layered anti-symmetric ply-orientation $(\pm\theta^o)_2$ and the load bandwidth ratio η on the stability behaviour of a unidirectional loaded square plate with a central single stiffener [refer Figure 6 (a)] for S-S-S-S and C-C-C-C edged stiffened plates are depicted in Figures 8 (a) and (b), respectively. It is noticed from Figure 8 (a) that the buckling resistance is generally found to be maximum for a plate with $(\pm30^o)_2$ layup irrespective of the values of η. This may be attributed to the higher flexural stiffness of the anti-symmetric stiffened plate with $(\pm30^o)_2$ layup. Similarly, it is noticed from Figure 8 (b) that the critical load is found to be maximum for ply-orientations between $(\pm30^o)_2$ and $(\pm40^o)_2$ depending on values of η for the C-C-C-C edged stiffened plate. From these two figures, it is also inferred that the buckling load generally increases with increase in the value of η. This may be due to the fact that the contribution of the stiffener in resisting critical load increases as the line of action of the resultant load approaches the stiffener center line. It may be stated that the stiffened plate with around $(\pm30^o)_2$ layup can be a better choice for this type of loading condition.

Similar studies are carried out for the same plate with biaxial edge loading and centrally placed biaxial stiffeners [refer Figure 6 (b)] and the results are depicted in Figures 9 (a) and (b). In Figure 9 (a), it is noticed that the buckling load steadily increases to a maximum as the ply-orientation varies from $(\pm0^o)_2$ to $(\pm30^o)_2$ and starts decreasing from $(\pm30^o)_2$ to $(\pm45^o)_2$. As the value of ply-orientation increases from $(\pm45^o)_2$ to $(\pm60^o)_2$, the critical loads again continue to increase to their maximum values. From $(\pm60^o)_2$ to $(\pm90^o)_2$, the critical loads are found to decrease to a minimum. This wavy variation is symmetrical in nature and the maximum buckling values are found at both $(\pm30^o)_2$ and $(\pm60^o)_2$ ply-angles.

Similarly, it can be noticed in Figure 9 (b) that the critical loads monotonically increases as the value of ply-orientation is increased from $(\pm0^o)_2$ to $(\pm45^o)_2$ and decreases from $(\pm45^o)_2$ to $(\pm90^o)_2$. The decreasing trend of critical loads from $(\pm30^o)_2$ to $(\pm45^o)_2$ to an intermediate value as observed in Figure 9 (a) is not reflected in this case, i.e. wavy variation does not exist in the C-C-C-C edged stiffened plate. It may be attributed to the fact that the edge rotational restraint increases the stiffness of the stiffened plate predominantly and hence the critical loads continue to increase for all values of η as seen in Figure 9 (b). For this kind of loading, the stiffened plate with $(\pm30^o)_2$ or $(\pm60^o)_2$ layup may be more useful for S-S-S-S edge conditions and the stiffened plate with $(\pm45^o)_2$ layup may be a better choice for C-C-C-C edge conditions.
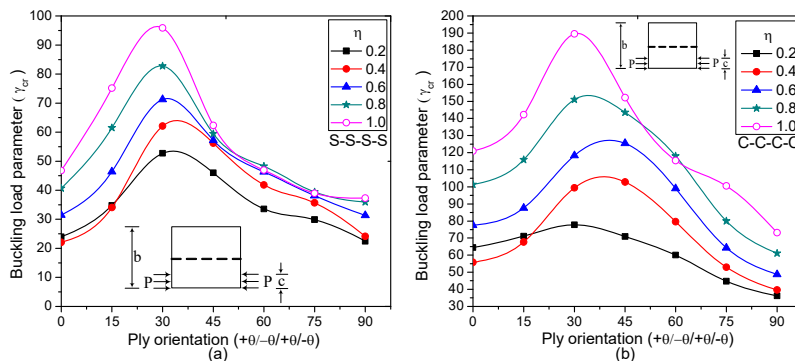

Figure 8: Variation of γ_{cr} with different ply-orientation (a) for simply supported and (b) for clamped square plate with centrally placed single stiffener ($\delta = 0.1$ and $\beta = 10$) under unidirectional partial edge loading from one edge.
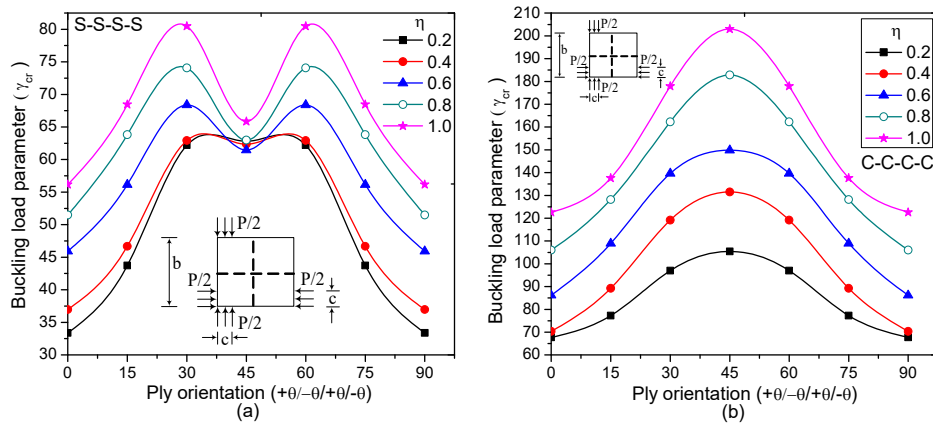
Figure 9: Variation of γ_{cr} with different ply-orientation (a) for simply supported and (b) for clamped square plate with central orthogonal stiffeners ($\delta = 0.1$ and $\beta = 10$) under bidirectional partial edge loading from one edge.

3.5.3 Laminated Stiffened Plate under Uniaxial and Biaxial Partial Edge Loading from Both Edges

The effect of load case shown in Figure 6(c) on the critical loads of unidirectional stiffened plate is examined and the results are depicted in Figures 10 (a) and (b) for different ply-orientations and boundary conditions (S-S-S-S, C-C-C-C). The buckling load is found to be maximum at $(\pm 30^{o})_2$ layup irrespective of the values of η as can be seen in Figure 10 (a). The same phenomenon has been observed in Figure 8 (a), the possible reason being that the effect of loading from one edge [Figure 6 (a)] holds true for loading from both edges [Figure 6(c)]. Further, it is interesting to mention that for a particular ply-angle of about $(\pm 48^{o})_2$, the critical loads are practically same irrespective of the values of η, and similar phenomenon is again observed at $(\pm 90^{o})_2$ ply-angle in Figure 10 (a). The buckling behaviour of C-C-C-C edged stiffened plate, as shown in Figure 10 (b), is almost similar to that of S-S-S-S edged stiffened plate. However, in this case, the critical loads are independent of the value of η for only one particular ply-orientation, i.e. at $(\pm 90^{o})_2$.

The variation of critical loads for the bidirectional loaded square plate with bidirectional stiffeners [refer Figure 6 (d)] is now investigated and the results are presented in Figures 11 (a) and (b) for S-S-S-S and C-C-C-C edge conditions, respectively. The wavy variation of buckling loads observed in Figure 11 (a) is similar as that observed in Figure 9 (a). In both the cases, it is observed that the curves have two peaks, i.e. at $(\pm 30^{o})_2$ as well as $(\pm 60^{o})_2$ layups. Therefore, it is appropriate to choose the stiffened plate with either of these layups for these types of loading cases. The buckling variation of a stiffened plate with C-C-C-C edge condition is shown in Figure 11 (b). The variation is slightly different when compared to the one shown in Figure 9 (b). In this case, the curves for $\eta = 0.2$ to 0.6 have double peaks, i.e. at $(\pm 30^{o})_2$ and $(\pm 60^{o})_2$ ply-angles and beyond $\eta = 0.6$, the curves are having a single peak at $(\pm 45^{o})_2$ ply-angle. However, in this case, the choice of ply-orientation is purely dependent on the width of edge compression. For this type of loading, the stiffened plate with $(\pm 45^{o})_2$ layup may be suitable for $\eta = 0.8 - 1.0$, whereas, for the remaining values of η, the stiffened plate with $(\pm 30^{o})_2$ or $(\pm 60^{o})_2$ layup may be an appropriate choice.
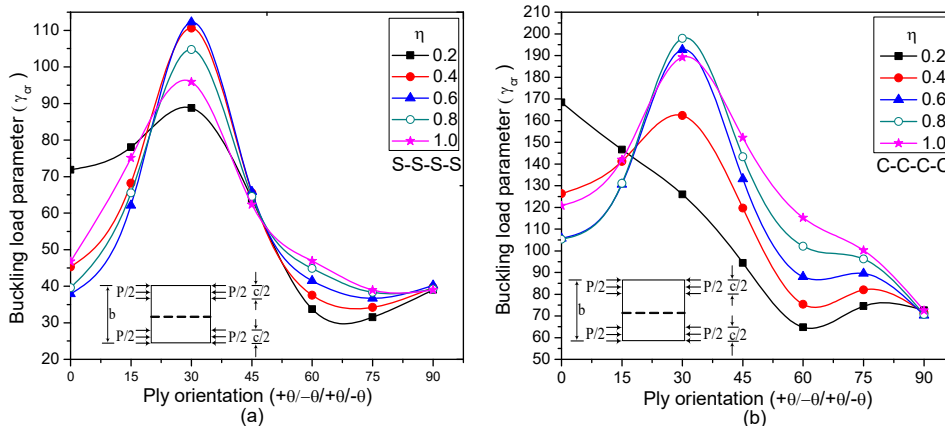
Figure 10: Variation of γ_{cr} with different ply-orientation (a) for simply supported and (b) clamped square plate with centrally placed single stiffener ($\delta = 0.1$ and $\beta = 10$) under unidirectional partial edge loading from both edges.
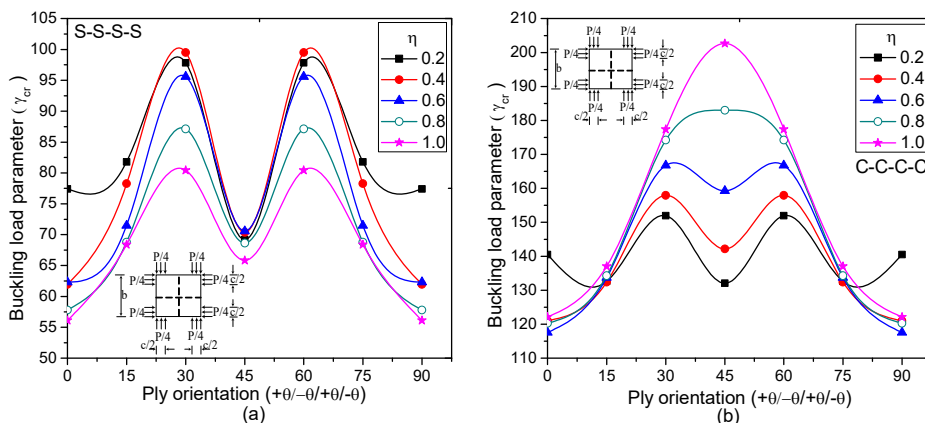

Figure 11: Variation of γ_{cr} with different ply-orientation (a) for simply supported and (b) for clamped square plate with centrally placed orthogonal stiffeners ($\delta = 0.1$ and $\beta = 10$) under bidirectional partial edge load from both edges.

3.5.4 Laminated Stiffened Plate with Uniaxial and Biaxial Partial Edge Loading at the Center

The variation of γ_{cr} with the ply-orientation angles $(\pm\theta^{\circ})_2$ for S-S-S-S and C-C-C-C square plate with a centrally placed single stiffener subjected to uniaxial loading [refer Figure 6 (e)] is shown in Figures 12 (a) and (b). It is noticed from Figure 12 (a) that, in general, the critical load γ_{cr} is maximum for a ply-angle of $(\pm30^{\circ})_2$ except for lower values of η. Further, the variation of buckling load after $(\pm55^{\circ})_2$ ply-orientations is not significant with respect to η. Similar behaviour can also be observed in a C-C-C-C edged stiffened plate as shown in Figure 12 (b). However, in this case, the buckling variation is not significant after $(\pm75^{\circ})_2$ ply-orientation for all values of η.

Similar studies are carried out for the same plate with a centrally placed biaxial stiffener and biaxial loading conditions and the results are depicted in Figures 13 (a) and (b). The study indicates that the critical load generally increases with an increased value of η. It may be due to increasing of higher edge restraints as the width of load increases towards the corner of the plate.

However, in case of S-S-S-S edged stiffened plate as shown in Figure 13 (a), the critical load γ_{cr} is found to be maximum for both $(\pm 30^\circ)_2$ and $(\pm 60^\circ)_2$ ply-orientations only for higher values of η. However, the maximum shifts towards $(\pm 20^\circ)_2$ and $(\pm 70^\circ)_2$ ply-orientations as the value of η decrease towards $\eta = 0.2$. To sum up, the buckling behaviour with the wavy variation of this case is almost similar to the case shown in Figure 9 (a). The buckling variation of C-C-C-C edged stiffened plate as shown in Figure 13 (b) displays similar behaviour when compared to the one shown in Figure 11 (b). For this type of loading and edge conditions, $(\pm 45^\circ)_2$ ply-angle shows a higher buckling resistance for all values of η except $\eta = 0.1$.
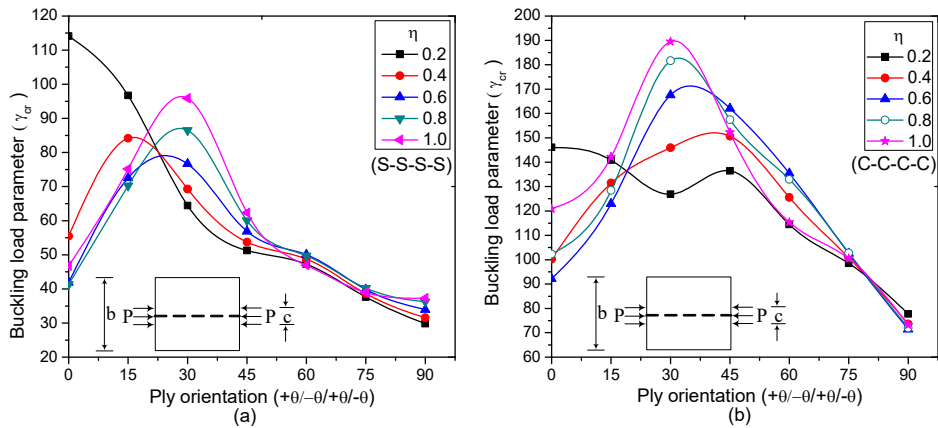

Figure 12: Variation of γ_{cr} with different ply-orientation (a) for simply supported and (b) for clamped square plate with centrally placed single stiffener ($\delta = 0.1$ and $\beta = 10$) under uniaxial partial edge load from the center of the plate.
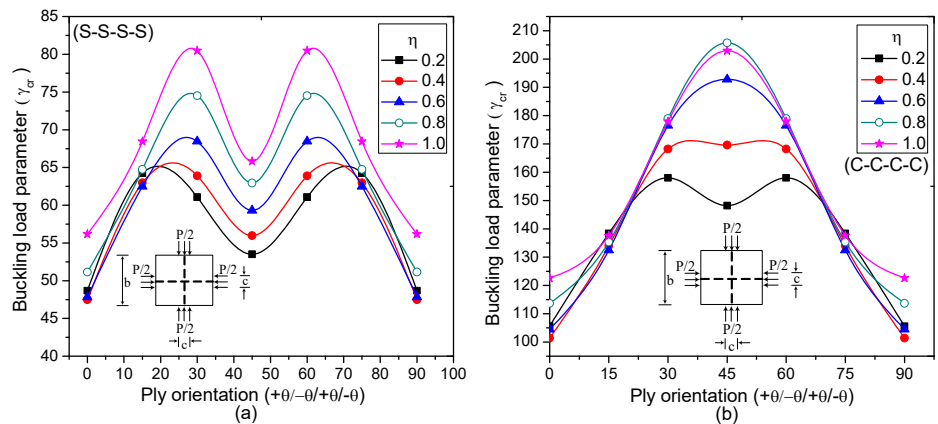

Figure 13: Variation of γ_{cr} with different ply-orientation (a) for simply supported and (b) for clamped square plate with centrally placed orthogonal stiffeners ($\delta = 0.1$ and $\beta = 10$) under bidirectional partial edge load from the center.

4   CONCLUSION

The results from the present investigation of the vibration and stability characteristics of S-S-S-S and C-C-C-C edged angle-ply stiffened plate under a variety of partial edge compressions can be summarized as follows:

1. It is found that for any particular ply-orientation and loading condition, the vibration frequency decreases as the intensity of edge load increases and becomes zero at the corresponding critical loads.
2. For a plate with a single stiffener subjected to unidirectional partial edge loading (extending from one edge and both edges), the critical load is found to be maximum at around $(\pm 30^{o})_2$ layup irrespective of boundary conditions. The same phenomenon is also applicable for the centrally loaded stiffened plate only for higher values of η.
3. It is also noticed that the boundary conditions play a significant role in the stability behaviour of a stiffened plate under bidirectional partial edge loads. The stiffened plate with $(\pm 30^{o})_2$ and $(\pm 60^{o})_2$ layups show maximum buckling resistance for S-S-S-S edge condition irrespective of loading conditions. However, for C-C-C-C edge condition, the critical load is found to be maximum at $(\pm 45^{o})_2$ ply-orientation in the case of bidirectional load acting from one edge of the plate (un-symmetrical loading case). For the same C-C-C-C edged stiffened plate subjected to symmetrical biaxial loading, the critical loads are found to be maximum at $(\pm 45^{o})_2$ ply-angle only for higher η.
4. It is interesting to note that when an S-S-S-S edged stiffened plate is subjected to a unidirectional edge load acting from both edges, the critical buckling loads are found to be practically same at an ply-angle of $(\pm 48^{o})_2$ irrespective of load bandwidth ratio η. This phenomenon is again observed at $(\pm 90^{o})_2$ ply-orientation. However, a similar trend is observed in C-C-C-C edged stiffened plate only at a ply-orientation of $(\pm 90^{o})_2$.

Acknowledgements

References

Bathe, K.J. (1996). Finite element procedures, Prentice Hall, Englewood Cliffs.

Butalia, T.S., Kant, T., Dixit, V.D., (1990). Performance of heterosis element for bending of skew rhombic plates. Computers and Structures 34(1): 23-49.

Deolasi, P.J., Datta, P.K., Prabhakar, D.L., (1995). Buckling and vibration of rectangular plates subjected to partial edge loading (compression or tension). Journal of Structural Engineering 22(3): 135-144.

Hamedani, S.J., Khedmati, M.R., Azkat, S., (2012). Vibration analysis of stiffened plates using finite element method. Latin American Journal of Solids and Structures 9(1): 1-20.

Hamedani, S.J., Ranji, A.R., (2013). Buckling analysis of stiffened plates subjected to non-uniform biaxial compressive loads using conventional and super finite elements. Thin-Walled Structures 64 41-49.

Hashemi, S.H., Khorshidi, K., Amabili, M., (2008). Exact solution for linear buckling of rectangular Mindlin plates. Journal of Sound and Vibration 315(1): 318-342.

Hinton, E., Owen, D.R.J. (1984). Finite element software for plates and shells, Pineridge Press, Swansea, U.K.

Hughes, T.J.R., Cohen, M., (1978). The "heterosis" finite element for plate bending. Computers and Structures 9(5): 445-450.

Jana, P., Bhaskar, K., (2006). Stability analysis of simply-supported rectangular plates under non-uniform uniaxial compression using rigorous and approximate plane stress solutions. Thin-Walled Structures 44(5): 507-516.

Kaldas, M.M., Dickinson, S.M., (1981). Vibration and buckling calculations for rectangular plates subject to complicated in-plane stress distributions by using numerical integration in a Rayleigh-Ritz analysis. Journal of Sound and Vibration 75(2): 151-162.

Kamruzzaman, M., Umar, A., Naqvi, S.Q.A., Siddiqui, N.A., (2006). Effect of composite type and its configuration on buckling strength of thin laminated composite plates. Latin American Journal of Solids & Structures 3(3): 279-299.

Khedmati, M.R., Edalat, P., (2010). A numerical investigation into the effects of parabolic curvature on the buckling strength and behaviour of stiffened plates under in-plane compression. Latin American Journal of Solids and Structures 7(3): 249-264.

Kolli, M., Chandrashekhara, K., (1996). Finite element analysis of stiffened laminated plates under transverse loading. Composites science and technology 56(12): 1355-1361.

Leissa, A.W., Ayoub, E.F., (1988). Vibration and buckling of a simply supported rectangular plate subjected to a pair of in-plane concentrated forces. Journal of Sound and Vibration 127(1): 155-171.

Mirzaei, S., Azhari, M., Bondarabady, H.A.R., (2015). On the use of finite strip method for buckling analysis of moderately thick plate by refined plate theory and using new types of functions. Latin American Journal of Solids and Structures 12(3): 561-582.

Mukhopadhyay, M., Mukherjee, A., (1990). Finite element buckling analysis of stiffened plates. Computers and Structures 34(6): 795-803.

Palani, G.S., Iyer, N.R., Appa Rao, T.V.S.R. (1989) Studies on the performance of isoparametric finite elements for static and vibration analysis of beams and plates. Project Report No SST-RR-88-2, Structural Engineering Research Center, Madras.

Palani, G.S., Iyer, N.R., Rao, T.V.S.R., (1992). An efficient finite element model for static and vibration analysis of eccentrically stiffened plates/shells. Computers & Structures 43(4): 651-661.

Pugh, E.D.L., Hinton, E., Zienkiewicz, O.C., (1978). A study of quadrilateral plate bending elements with 'reduced'integration. International Journal for Numerical Methods in Engineering 12(7): 1059-1079.

Reddy, J.N. (1996). Mechanics of laminated composite plates, CRC press, New York.

Reddy, J.N., Phan, N.D., (1985). Stability and vibration of isotropic, orthotropic and laminated plates according to a higher-order shear deformation theory. Journal of Sound and Vibration 98(2): 157-170.

Sahu, S.K., Prabhakar, D.L., Datta, P.K., (2001). Vibration and buckling of laminated composite plates subjected to non-uniform in-plane edge loading. Journal of Structural Engineering 28(2): 75-80.

Satish Kumar, Y.V., Mukhopadhyay, M., (2000). A new triangular stiffened plate element for laminate analysis. Composites Science and Technology 60(6): 935-943.

Sayyad, A.S., Ghugal, Y., (2014). Buckling and free vibration analysis of orthotropic plates by using exponential shear deformation theory. Latin American Journal of Solids and Structures 11(8): 1298-1314.

Sayyad, A.S., Shinde, B.M., Ghugal, Y.M., (2016). Bending, vibration and buckling of laminated composite plates using a simple four variable plate theory. Latin American Journal of Solids and Structures 12(2): 1-20.

Singh, S., Kulkarni, K., Pandey, R., Singh, H., (2012). Buckling analysis of thin rectangular plates with cutouts subjected to partial edge compression using FEM. Journal of Engineering design 10(1): 128-142.

Singh, S.K., Chakrabarti, A., (2012). Buckling analysis of laminated composite plates using an efficient C0 FE model. Latin American Journal of Solids and Structures 9(3): 1-13.

Sommerfield, A., (1906). Über die Knicksicherheit der Stege von Walzwerkprofilen. Z Math Phys 54 113-153.

Srivastava, A.K.L., Datta, P.K., Sheikh, A.H., (2003). Buckling and vibration of stiffened plates subjected to partial edge loading. International Journal of Mechanical Sciences 45(1): 73-93.

Sundaresan, P., Singh, G., Rao, V., (1998). Buckling of moderately thick rectangular composite plates subjected to partial edge compression. International Journal of Mechanical Sciences 40(11): 1105-1117.

Thinh, T.I., Khoa, N.N., (2008). Free vibration analysis of stiffened laminated plates using a new stiffened element. Technische Mechanik 28(3): 227-236.

Thinh, T.I., Quoc, T.H., (2008). Analysis of stiffened laminated composite plates by finite element based on higher-order displacement theory. Vietnam Journal of Mechanics 30(2): 112-124.

Timoshenko, S.P., Gere, J.M. (1961). Theory of elastic stability, McGraw-Hill, New York.

Xiao, J.R., Gilhooley, D.F., Batra, R.C., Gillespie Jr, J.W., McCarthy, M.A., (2008). Analysis of thick composite laminates using a higher-order shear and normal deformable plate theory (HOSNDPT) and a meshless method. Composites Part B: Engineering 39(2): 414-427.

Yamaki, N., (1953). Buckling of a rectangular plate under locally distributed forces applied on the two opposite edges. Report of the Institute of High Speed Mechanics, Tohoku Univerity, Japan 26 71-87.